

# Simulations on the number of entanglements of a polymer network using knot theory

W. Michalke, M. Lang, S. Kreitmeier,\* and D. Göritz

University of Regensburg, Institute for Experimental and Applied Physics, Polymer Physics, 93040 Regensburg, Germany

(Received 08 September 2000; published 13 June 2001)

Polymer networks, created on the computer using the Bond-Fluctuation-Algorithm, offer the possibility to count the number of entanglements. We generated networks consisting of 5000 chains that were cross linked at their end groups via tetra-functional cross linkers. The analysis of the topology was performed by computing the Homfly polynomial of the entanglements offering a much more precise determination of the knot and entanglement type than the Gaussian linking number. It also allows us to determine the influence of Brunnian links. Results concerning the connection between the chain length and the number of entanglements are shown.

DOI: 10.1103/PhysRevE.64.012801

PACS number(s): 36.20.-r, 83.10.Rs, 61.41.+e

## I. INTRODUCTION

Structural properties play an important role in understanding the mechanical behavior of polymer systems. The role of entanglements, in particular, during the deformation process is still not exactly understood—it is known that topological links exist besides the chemical cross links, but their amount and type is unknown. Since the works of Vologodskii *et al.* [1,2], who determined the knot types formed in simulations of ring-shaped single polymer chains using the Alexander polynomial, a lot of work was done in determining the topology of DNA [3,4] and of simple polymer systems [5–10] with the Alexander polynomial. In our approach, we determine the link types of the entanglements of a polymer network using the Homfly polynomial [11], which can distinguish the different knot and link types with a much higher precision. We will thus be able to give a good prediction for the number of topological links per mesh of polymer networks with differing precursor chain length. In Sec. II, we introduce the simulation algorithm used to obtain our results. In Sec. III, we show how to apply knot theory to determine the entanglement types. The results of the investigations are reported in Sec. IV.

## II. SIMULATION ALGORITHM

The algorithm used for creating polymer networks is the bond-fluctuation algorithm, first introduced in Ref. [12]. It works as follows: The monomers are represented by cubes occupying eight sites on a lattice. They are connected by a set of 108 bond vectors that correspond to Kuhn segments. The choice of the bond vectors ensures that the self avoidance of the monomers automatically implies the cut avoidance of the bonds. Dynamics are obtained by random jumps of the monomers of one lattice unit. After polymerization, we relaxed the melt up to equilibrium. After that, a stoichiometric number of tetrafunctional cross linkers is inserted in the melt. Whenever a cross linker is in next-neighbor distance to a chain end it attaches to it and further diffuses together with the chain until it is attached to four chain ends

[13]. We stopped the reaction at a 95% conversion ratio due to a pronounced slow down in the cross-linking process. The characteristics of the simulated systems are summarized in Table I. For the networks N11-N38 we built three independent networks. Due to only small differences present, we show one representative network here.

The main parameter varied was the precursor chain length ranging between 11 and 241 monomers per chain. The number of chains was mostly 5000, chosen in order to get good statistics. The overall number of monomers in the system varied between 150 000 and 1 250 000. We performed simulations with an occupation density of 64% (labeled with  $N$ ) and 46% (labeled with  $A$ ) as a prefix to the chain length. The last two rows denote the overall number of meshes and the average number of chains per mesh for the different networks.

## III. ANALYSIS OF ENTANGLEMENTS USING KNOT THEORY

In order to compute the type of the entanglements, it is necessary to find a decomposition of the network into meshes. The algorithm used for obtaining a decomposition is described in detail in Ref. [14]. Since small meshes will first hinder the deformation, the goal was to find a spanning tree for which the sum of lengths of the meshes is minimal. By applying weightings to the chains and optimizing the order of adding chains to the tree one obtains a decomposition into the meshes contributing most to the strain during the deformation process.

A method frequently used to study the topology of poly-

TABLE I. Overview of the simulated networks. “occ. dens.” hereby refers to the occupation density in monomers while “ch./mesh” denotes the average ratio of chains per mesh for the networks.

Networks	N11	N27	N38	N81	N241	A10	A20	A80
Chains	17128	5418	5116	5418	5176	10560	5280	5280
X-linkers	8564	2709	2558	2709	2588	5280	2640	2640
Occ. dens.	0.64	0.64	0.64	0.64	0.63	0.48	0.47	0.46
Meshes	6916	2200	2067	2200	2093	4534	2055	2125
Ch./mesh	6.15	6.43	6.68	7.15	7.70	5.71	6.18	6.90

\*Electronic address:

stefan.kreitmeier@physik.uni-regensburg.de

TABLE II. Frequency of occurrence of the simplest prime and factor knots for the different networks. The symbol # refers to the product of the two knots.

Networks	No of meshes	$3_1$	$4_1$	$5_1$	$5_2$	$>5$	$3_1\#3_1$	$3_1\#4_1$
A10	4533	4	0	0	0	0	0	0
N11	6918	15	0	0	0	0	0	0
A20	2049	8	1	0	0	0	0	0
N27	2203	41	4	0	0	0	0	0
N38	2069	60	5	0	0	3	0	1
A80	2125	132	8	2	6	4	0	0
N81	2200	185	23	12	7	4	1	2
N241	2093	468	97	22	41	91	37	26

mer networks is the Gaussian linking number (GLN) introduced to polymers in [15,16]. It was immediately attacked by Vologodskii *et al.* [1] as being inadequate, but remained an often-used method for characterizing links [17–20]. In fact, the GLN has serious shortcomings that restrict its applicability to networks with short chains where only the simplest types of entanglements occur. It can, in detail, only detect two-component links, gives almost no information about the topological shape, and even simple links such as the Whitehead link  $5_2^2$  are not detected. Therefore, we used the Homfly Polynomial to gain more precise information. In order to be able to calculate it, several steps have to be performed. The entanglements as present in the networks often have several hundreds of crossings. We thus used the reduction algorithm proposed by Ref. [21] to perform a triangle reduction of the chains. This decreased the number of crossings in the resulting graph to less than 20% of the original number. As a second step, one has to find a projection that both contains as few crossings as possible and in which no vertex lies in the same projection direction as a line. This was achieved by choosing the best out of 50 random projections of the entanglement on a unit sphere resulting in a further reduction of 70%.

We first investigated the Alexander polynomial using an improved version of the Vologodskii algorithm that has the advantage of a faster computation in order to eliminate trivial knots and links from the set of entanglements. As a side effect of the computation of the Alexander polynomial, the GAUSS code for the entanglements was determined. The calculation of the Homfly polynomial from the GAUSS code was performed using the program of Gouesbet *et al.* [22], who calculate it using a skein-template algorithm. The GAUSS code of a link, as well as the computation algorithm, are described in detail in their paper. An algorithm for the analysis of the polynomials determined the type for all knots with up to 10 crossings, all prime links with up to 9 crossings and all factor links with up to 11 crossings. For links with identical Homfly polynomial, the link with the fewer number of crossings was assigned. The number of links where no link type could be assigned was small for all networks with the exception of N241. Here, 1/3 of the polynomials could not be associated with a link type. Two reasons are responsible for this fact. First, we restricted our investigations to links

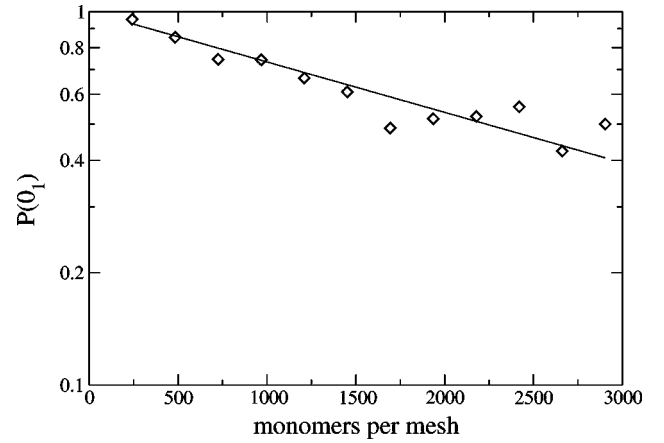


FIG. 1. Semilogarithmic plot of the probability of a mesh to form a trivial knot versus the precursor chain length.

with a number of crossings smaller than 41 after reduction due to a steep increase of the computation time for the Homfly polynomial. Second, prime links with a higher number of crossings than nine in the minimal projection could not be detected.

#### IV. RESULTS

We first present the results concerning single meshes. Table II shows the probabilities of the different knot types for the networks simulated.

As expected, the meshes of the network N11 almost solely form a simple loop. In contrast, 37% of all meshes of network N241 already form a nontrivial knot. The probabilities for the networks of lower density are significantly lower for all knot types. The relative probabilities of the knot types show a rapid decrease with increasing number of crossings. When comparing the relative probabilities of the different knot types with the same number of crossings, one obtains results comparable with Ref. [5]. For example, the probability to form the knot  $5_2$  is twice as high as for the knot  $5_1$  in network N241.

Drawing the probability of forming a nontrivial knot against the precursor chain length in a semilogarithmic plot an exponential decrease shows up (Fig. 1).

The fit is of the form  $P(N) = \exp(-N/N_0)$  with  $N_0$

TABLE III. Frequency of occurrence of the simplest prime links. Link types with up to 9 crossings could be detected.

Networks	$2_1^2$	$4_1^2$	$5_1^2$	$6_1^2$	$6_2^2$	$6_3^2$	$>6$
A10	3632	38	3	0	0	0	0
N11	9887	190	7	2	2	1	1
A20	3973	98	12	4	0	1	0
N27	8448	388	35	7	5	15	34
N38	12187	768	83	21	22	34	67
A80	16579	1969	408	112	94	105	386
N81	23796	3259	770	184	203	207	896
N241	20846	4348	1598	548	442	615	3745

TABLE IV. Frequency of occurrence of the simplest nonprime links. Link types with up to 11 crossings could be detected.

Networks	$3_1$ and $0_1$	$3_1$ and $3_1$	$4_1$ and $0_1$	$3_1$ and $4_1$	$5_1$ and $0_1$	$5_2$ and $0_1$	$>5$
A10	4	0	0	0	0	0	0
N11	40	0	0	0	0	0	0
A20	20	0	0	0	0	0	0
N27	421	10	2	7	0	7	4
N38	736	20	20	4	0	23	46
A80	2309	100	148	12	32	114	59
N81	4424	346	621	159	183	127	173
N241	16 741	2918	3337	2157	682	1175	3880

=3219. This is in good agreement with simulations of Koniaris and Muthukumar [7], who found an exponent of  $N_0 = 2400$  in a rod-bead model with a bead radius of  $r=0.2$  that is roughly comparable with the bond-fluctuation model. However due to the comparatively small chain length, a linear fit still yields a good approximation as well.

A summary of the results concerning links is presented in Table III.

It gives the probabilities of the most frequent prime link types for all networks investigated. The simple Hopf-link  $2_1^2$  plays a dominant role for all networks simulated. The frequency of occurrence again rapidly decreases with increasing number of crossings. Interestingly, network N241 has a decreasing number of Hopf links compared with network N81. This fact indicates that higher link types and especially nonprime links play an important role for large networks as also pointed out by Table IV.

Table IV presents the analogous results for nonprime links. The notation, e.g.,  $3_1$  and  $3_1$  means that two knots of type  $3_1$  are entangled in the form of a Hopf-link  $2_1^2$  with  $3_1$  knots as the components. For the small networks, almost all links are prime links. With increasing chain length, the nonprime links get more important and already contribute the major part for N241.

In Fig. 2, the number of topological links per mesh is

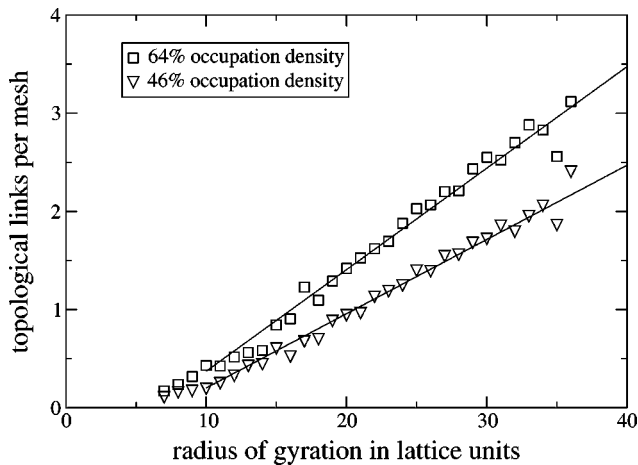


FIG. 2. Dependency of the number of topological links per mesh versus the radius of gyration for the network N81.

plotted via the radius of gyration for the networks A80 and N81, showing a linear increase both for low- and high-occupation density with a higher slope for the high-density network. The largest meshes form three topological links on the average.

In Fig. 3, the number of topological links per mesh for the networks with high-occupation density is plotted.

The triangles refer to the number of links obtained when assuming that one entanglement only forms one topological link, namely the Hopf-link  $2_1^2$ . The squares present the results when taking into account that higher link types can form several topological links per entanglement. Both show an almost linear increase with the precursor chain length. While only few links occur for the network N11, each mesh already forms more than four topological links for the network N241. The slope for network N241 is slightly lower than for the other networks. This might be due to an increasing number of meshes from nontrivial knots diminishing the radius of gyration of the meshes.

In computing the ratio between the number of topological links versus the number of chemical cross links, one finds that while the number of chemical cross links is much higher for network N11, the opposite is true for network N241. Here, 80% of the links are topological, while only 20% are chemical.

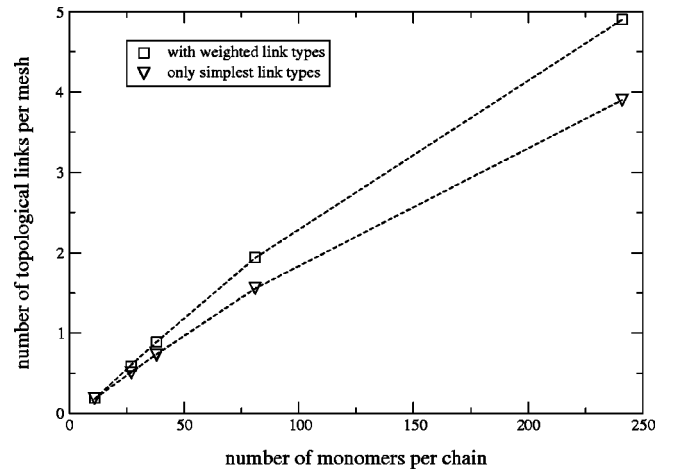


FIG. 3. Additional topological links per mesh for the networks with 64% occupation density.

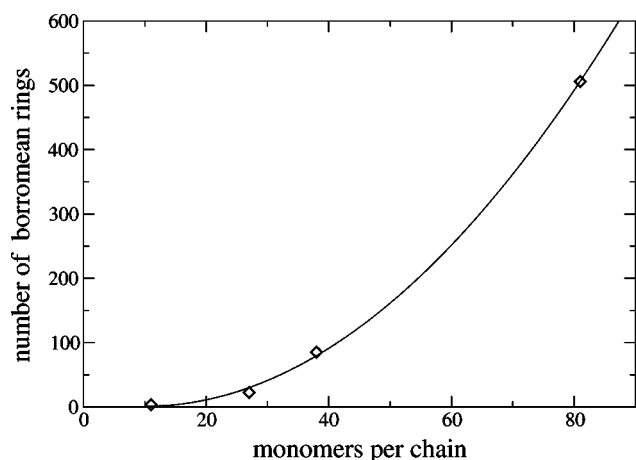


FIG. 4. Absolute number of Borromean rings found in the networks N11, N27, N38, and N81.

Finally we show the results obtained for Borromean rings. It is the simplest Brunnian link, for which no two components are entangled, but all together form a link. Figure 4 presents the number of Borromean rings for the networks N11 to N81.

A rapid increase in the number of occurrences is found. In the network N81, every fourth mesh is part of a Borromean ring. The graph shows a quadratic fit  $P(x) = a + bx + cx^2$  for the data with the parameters  $a = 11.014$ ,  $b = -2.001$ , and  $c = 0.10021$ . However, due to the small chain length, an exponential fit is also possible. The increase indicates that Brun-

nian links play a non-negligible role in counting the number of entanglements for large networks.

## V. SUMMARY

The investigations performed aimed at giving a good prediction for the number of topological links in a network. After creating a network in the computer, we decomposed it into small meshes. The analysis of the entanglements was performed using the Homfly polynomial ensuring a very high precision for the determination of link types. We found an exponential decrease of the probability of a trivial knot to be found versus the chain length. Concerning links, a linear increase of the number of topological links per mesh was obtained when plotted both versus the radius of gyration and the precursor chain length. For the network N241, a significant number of entanglements form two or more topological links. The ratio between the number of topological links and the number of chemical cross links raised up to 4:1 for network N241. Finally, a quadratic increase of the number of Borromean rings with the precursor chain length was obtained.

## ACKNOWLEDGMENTS

The authors would like to thank Mr. Meunier-Guttin-Cluzel for providing us with his program for determining the Homfly polynomials. Wolfgang Michalke wishes to thank the Deutsche Forschungsgemeinschaft for financial support (GO 287/26-1).

- 
- [1] V. Vologodskii, A.V. Lukashin, M.D. Frank-Kamenetskii, and V.V. Anshelevich, Zh. Éksp. Teor. Fiz. **66**, 2153 (1974) [Sov. Phys. JETP **39**, 1059 (1974)].
  - [2] V. Vologodskii, A.V. Lukashin, and M.D. Frank-Kamenetskii, Zh. Éksp. Teor. Fiz. **67**, 1875 (1974) [Sov. Phys. JETP **40**, 932 (1975)].
  - [3] T. Schlick and W.K. Olson, Science **257**, 1110 (1992).
  - [4] B. Maier and J.O. Rdlr, Phys. Rev. Lett. **82**, 1911 (1999).
  - [5] J.P.J. Michels and F.W. Wiegel, J. Phys. A **22**, 2393 (1989).
  - [6] E.J.J. van Rensburg and S.G. Whittington, J. Phys. A **23**, 3573 (1990).
  - [7] K. Koniaris and M. Muthukumar, Phys. Rev. Lett. **66**, 2211 (1991).
  - [8] E.J.J. van Rensburg, D.A.W. Sumners, E. Wasserman, and S.G. Whittington, J. Phys. A **25**, 6557 (1992).
  - [9] E. Orlandini, M.C. Tesi, E.J.J. van Rensburg, and S.G. Whittington, J. Phys. A **29**, L299 (1996).
  - [10] E. Orlandini, M.C. Tesi, E.J.J. van Rensburg, and S.G. Whittington, J. Phys. A **31**, 5953 (1998).
  - [11] P. Freyd *et al.* Bull. Am. Math. Soc. **12**, 239 (1985).
  - [12] I. Carmesin and K. Kremer, Macromolecules **21**, 2819 (1988).
  - [13] H.L. Trautenberg, J.-U. Sommer, and D. Göritz, J. Chem. Soc., Faraday Trans. **91**, 2649 (1995).
  - [14] M. Lang, W. Michalke, S. Kreitmeier, and D. Göritz, Macromol. Theor. Simul. **10**, 204 (2001).
  - [15] S.F. Edwards, Proc. Phys. Soc. Jpn. **91**, 513 (1967).
  - [16] S.F. Edwards, J. Phys. A **1**, 15 (1968).
  - [17] M.G. Brereton and M. Filbrandt, Polymer **26**, 1134 (1985).
  - [18] K. Iwata and S.F. Edwards, J. Chem. Phys. **90**, 4567 (1989).
  - [19] R. Everaers and K. Kremer, Phys. Rev. E **53**, R37 (1996).
  - [20] R. Everaers, New J. Phys. **1**, 12.1 (1999).
  - [21] J.P.J. Michels, Comput. Phys. Commun. **44**, 289 (1987).
  - [22] G. Gouesbet, S. Meunier-Guttin-Cluzel, and C. Letellier, Appl. Math. Comput. **105**, 271 (1999).